PREFIRE Data User Guide

Level 2B Cloud Properties (2B-CLD)

Version R01
(20250331)

Nathaniel Miller
Erin Hokanson Wagner
Aronne Merrelli
Tim Michaels

Table of Contents

1 Introduction

This user guide contains information for the PREFIRE data collections PREFIRE_SAT1_2B-CLD and PREFIRE_SAT2_2B-CLD, which are archived by the Atmospheric Science Data Center (ASDC) at the NASA Langley Research Center. These collections contain cloud properties as retrieved from data collected by the PREFIRE Thermal Infrared Spectrometers (PREFIRE-TIRS).

1.1 Mission Overview

The Science Mission Directorate (SMD) at NASA Headquarters selected the Polar Radiant Energy in the Far InfraRed Experiment (PREFIRE) as an Earth System Science Pathfinder (ESSP) Earth Venture Instrument (EVI-4) class Mission of Opportunity. Through spectrally resolved observations of radiances spanning the radiatively significant portions of the Mid- and Far-InfraRed (MIR and FIR), PREFIRE addresses two complementary hypotheses:

1. Time-varying errors in both FIR surface emissivity and thermal radiation modulate estimates of energy exchanges between the surface and the atmosphere in the Arctic.
2. These terms are responsible for a large fraction of the spread in projected rates of change for Arctic surface, ocean, and atmosphere characteristics.

These hypotheses are addressed through five related objectives:

- O1.1 Quantify snow and ice FIR emissivity spectra and their variability on seasonal scales;
- O1.2 Quantify the FIR thermal radiation and its response to seasonal variations in cloud cover / water vapor;
- O1.3 Quantify variability in Arctic spectral surface emission and the thermal radiation across the FIR owing to transient cloud and water vapor and sub-daily surface phase-change processes;
- O2.2 Quantify thermal emission errors on projected rates of Arctic warming and sea ice loss;
- O2.3 Determine the impact of improved surface emissivity on modeled ice sheet dynamic processes on hourly scales.

PREFIRE uses broadband infrared (> 75% of surface emitted thermal radiation) radiance measurements made from the separate orbiting platforms (CubeSats) to address the science objectives. The PREFIRE payloads are two stand-alone instruments built at JPL using heritage from the Mars Climate Sounder and the Moon Mineralogy Mapper. The PREFIRE instruments are thermal infrared imaging spectro-radiometers with more than 50 spectral bands. Each PREFIRE instrument uses ambient temperature thermopile detectors and operates in a pushbroom mode with a point and stare mirror for viewing nadir (Earth), space, and a calibration target. PREFIRE data are calibrated with data from views of the internal calibration target and of space, which are viewed multiple times per orbit.

Soon after launch, the orbit altitude was approximately 531 km for both satellites. However, the PREFIRE CubeSats do not have station-keeping abilities and so their altitudes decrease with time. The current satellite altitude is recorded within the 2B-CLD data product files as the *sat_altitude* field (in the *Geometry* data group).

The PREFIRE project delivers space-based measurements of radiative fluxes, cloud masks, spectrally variant surface emissivity (ε_λ), and column water vapor (CWV). These are science products with the precision, resolution, and coverage needed to improve our understanding of polar energy balances and

Earth-system effects over diurnal and seasonal cycles at scales that capture surface and cloud variability. During its approximately one-year baseline mission, PREFIRE will capture the natural variability in Arctic and Antarctic CWV and surface temperature. PREFIRE reduces uncertainties in the surface and atmospheric components of the polar energy budget.

1.2 Data Overview

An optimal estimation approach, as described in Rodgers (2000), is used to provide the best estimate of the three state variables in the 2B-CLD data product: Cloud Top Pressure (CTP; *cloudtop_pressure* in the *Cld* data group), Cloud Optical Depth (COD; *cloud_tau*), and Cloud-particle Effective Diameter (CED; *cloud_d_eff*). Note that the retrieval of COD is done in logarithmic space, although the result and uncertainty are reported in linear space. A Levenberg-Marquardt parameter is used to adjust the relative weight of the prior information compared to information from the Level 1B Radiance (1B-RAD) measurements. For CTP, COD and CED the values for the respective first guesses are 600 hPa, 5.0, and 40 µm and the *a priori* uncertainties are 200 hPa for CTP, 20 µm for CED, and 3.16 for COD.

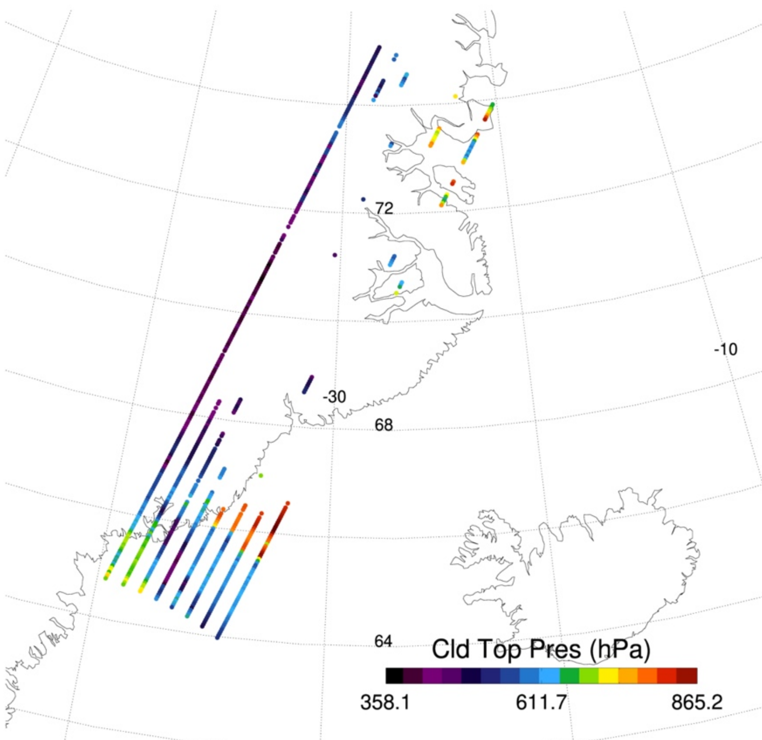

Figure 1-1. Cloud Top Pressure retrieved from PREFIRE-SAT2 data (segment of granule ID 00659) on 2024-07-07.

The forward model utilized in the retrieval algorithm, described in Lui et al. (2006), is the Principal Component-based Radiative Transfer Model (PCRTM). PCRTM contains ice and water cloud spectral emissivity models, although the 2B-CLD algorithm performs the retrieval specifically using the ice cloud model due to a lack of *a priori* microphysical information. The

Jacobians are calculated numerically using PCRTM via small perturbations in the state variables. Parameters such as profiles of various atmospheric constituents, temperature profiles, and surface temperature from the PREFIRE Auxiliary Meteorology (AUX-MET) product are used as input into PCRTM. A surface emissivity of 1.0 is assumed. All these geophysical scene parameters are held constant during the retrieval.

In addition to the AUX-MET product, the 2B-CLD algorithm also utilizes the 1B-RAD radiances and the Level 2B Cloud Mask (2B-MSK) as input. The retrieval is only performed in cases where the cloud mask determines there is cloud present. The threshold for this cloudy determination requires a cloud probability greater than 0.6, which are classified as "likely cloud" or "confidently cloud" in the 2B-MSK data product. The algorithm will only use radiances from channels in the 1B-RAD product where the *detector_bitflags* variable indicates reliable data. If the *detector_bitflags* (1B-RAD) for bit indices 0, 1, 3, 4, or 5 are set, then the appropriate channels are not used in the retrieval. Thus, the channel combinations used will vary between the two PREFIRE CubeSats and be unique for each scene, leading to a variable number of channels used per scene. Even so, redundancy of the information content across channels ensures an estimate and uncertainty is produced for every cloudy scene. In addition, if the (1B-RAD) *observation_quality_flag* is set to 2 ("bad"), then no retrieval is performed.

1.2.1 Spatial characteristics

The PREFIRE-TIRS instruments collect data continuously in a pushbroom mode, with an integration time of 0.7 seconds for each data frame. Each data frame contains a spectral measurement from each cross-track scene collected simultaneously. Within this continuous data collection, there are planned interruptions due to calibration cycles or data downlinks, and there are also occasional interruptions due to unplanned instrument operations changes or outages. Each calibration cycle takes ~18.7 seconds for PREFIRE-TIRS1 and ~9.7 seconds for PREFIRE-TIRS2, which implies a gap of approximately 27 and 14 data frames, respectively. Data downlinks create data gaps of up to 13 minutes, and the exact length varies.

Within the orbital swath there are eight distinct tracks of data associated with the eight separate spatial scenes for each PREFIRE-TIRS. The approximate scene footprint sizes are 11.8 km x 34.8 km (cross-track x along-track), with gaps between each scene of approximately 24.2 km. The swath itself is ~264 km across. Note that the scene footprint and swath sizes quoted here are for the orbit altitude soon after launch. However, the footprint size will slowly become smaller as the orbit altitude decreases with time. Do not assume constant footprint or swath dimensions.

PREFIRE-TIRS spatial footprints overlap each other in the along-track dimension. Assuming that no data are missing, any given point along the orbit swath will be observed by up to about 7 overlapping footprints in the along-track direction. The number of footprints that overlap a given footprint will slowly become smaller during the mission, as the satellites' orbital altitudes decrease. Do not assume an integer number of overlapping footprints.

A single data file or granule consists of data collected during approximately one orbit, beginning and ending near the equator to avoid granule borders over the polar regions. Data files are NetCDF4 format and approximately 20-30 MB in size. These data collections are archived at the ASDC DAAC and can be found at https://asdc.larc.nasa.gov/project/PREFIRE/PREFIRE_SAT1_2B-CLD_R01 and https://asdc.larc.nasa.gov/project/PREFIRE/PREFIRE_SAT2_2B-CLD_R01.

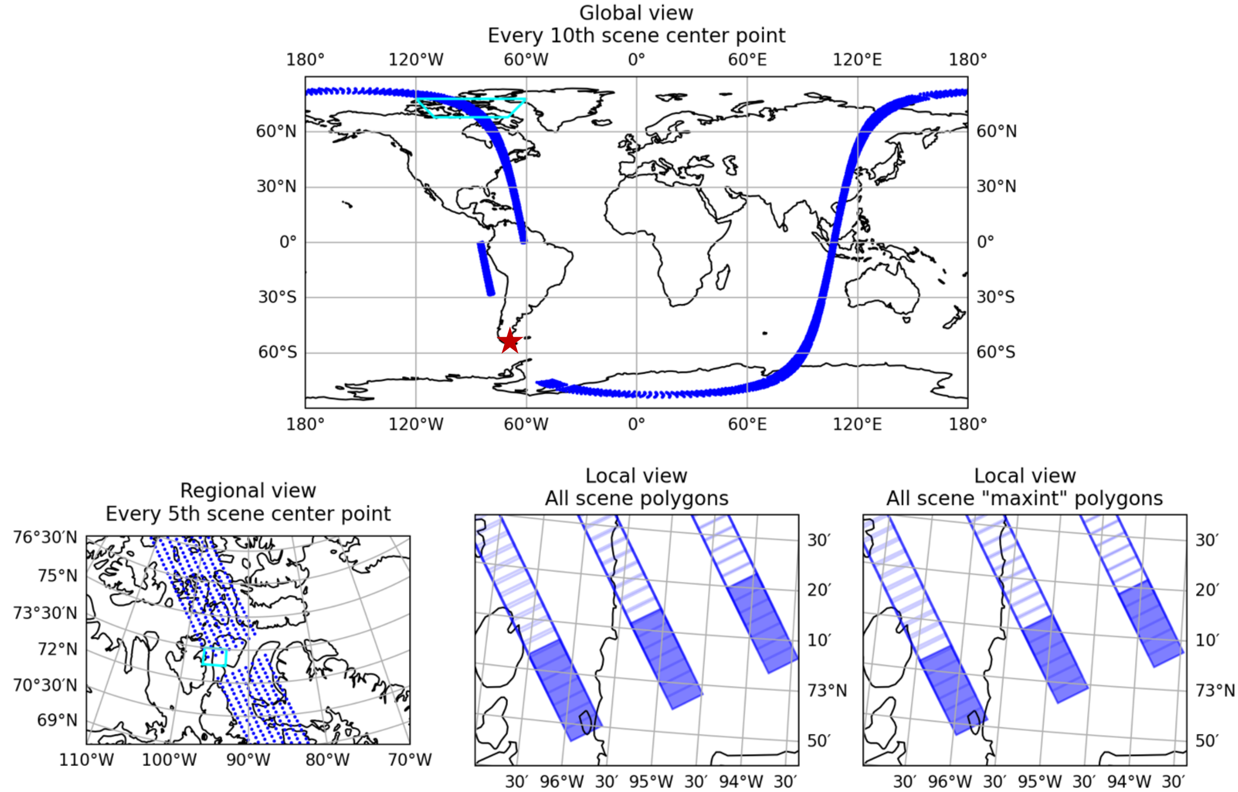

Figure 1-1. An example geolocated orbit (top panel) and focused regional and local plots (bottom panels). The global plot was selected to illustrate a data gap due to a data downlink at the Punta Arenas, Chile ground station, from approximately -70°S to -30°S on the ascending pass at the end of the granule. The zoomed in regional view (lower left) shows the data within the small cyan box in the global plot, and illustrates a smaller data gap due to instrument calibration. The local views (lower middle and right) show the actual scene ground footprint polygons, for the cyan box denoted in the regional view. The first scene's polygon is filled blue, to illustrate the shape of the full field of view (FOV) for one data integration. During the 0.7 second integration time, the satellite moves along track slightly more than 5 km, which means the leading and trailing edges of the instantaneous FOV have translated forward by the same amount. The lower right plot shows the "max integration" footprint polygon, which includes the interior portion of the scene footprint that was within the sensor field of view for the entire integration period.

1.3 Purpose

The purpose of the 2B-CLD product is to estimate the macro-physical properties of clouds, including cloud top pressure (CTP), cloud optical depth (COD), and cloud-particle effective diameter (CED). Within the context of the PREFIRE data flow, the primary use of the 2B-CLD product is to provide a coarse estimate of cloud top pressure and cloud optical depth for use in the 2B-FLX retrieval in cloudy conditions (as determined by the 2B-MSK product). The 2B-CLD cloud top pressure can be used to distinguish between low-, mid-, and high-altitude clouds, and optically thin, moderate, and thick clouds.

2 Product Description

2.1 Algorithm description

A short description of the Level 2B Cloud Properties (2B-CLD) algorithm is in Section 1.2 (above).

2.2 File Specifications

2.2.1 File naming convention

File names for this collection follow the following convention:

PREFIRE_SAT<*satID*>_<*productID*>_<*collectionVersion*>_<*internalProductVersion* > <*YYYYMMDDhhmmss*>_<*granuleID*>.nc

For example, a representative Level 2B Cloud Properties (2B-CLD) product granule collected by PREFIRE-SAT1 on June 1, 2024 would have the following filename:

PREFIRE_SAT1_2B-CLD_R01_P00_20240601185321_00123.nc

2.2.2 File format

PREFIRE 2B-CLD data product files are created in NetCDF4 format with standard metadata. These files can be read with standard NetCDF libraries available in all popular scripting languages and many data visualization programs.

2.2.3 Quality flag and bitflags conventions

Users who only need a simple summary of the calibration quality can consult the *cld_quality_flag* variable (in the *Cld* data group; Tables 2-1 and 2-4). To fully understand the conditions corresponding to a certain flag, users can consult the *cld_qc_bitflags* variable within the 2B-CLD data product granules.

Table 22-11. Cloud quality flag specification

cld_quality_flag value	Description
0	Good retrieval
1	Retrieval converged but did not meet quality check
2	Retrieval did not converge
3	Retrieval went out of range
-99	Retrieval not attempted (missing)

2.2.4 Variables

The variable specifications for this collection are described below, with one table devoted to each top-level data group in the NetCDF4 file: *Geometry*, *Cld*. Note that the *Geometry* group, including all variables, is propagated to every downstream Level 2 data product from the Level 1B Radiance product (1B-RAD).

2.2.5 Variable dimensions

A summary of all array dimensions is given in Table 2-2. The *xtrack* dimension is equal to the number of cross-track scenes (8, for both instruments), the *spectral* dimension is equal to the number of spectral channels (63, for both instruments), and the *atrack* dimension is equal to the number of along-track Earth observation data frames in the product. The number of along-track frames varies from orbit to orbit, depending on the timing of downlink contacts, calibration data, and other rarer events. Generally, the maximum is around 7700–7900 frames in one product file, with substantially fewer in granules containing downlinks or unplanned instrument/spacecraft events.

Table 2--2

Dimension	**Abbreviation**
Along-track	*atrack*
Cross-track	*xtrack*
State Vector 1	*statev1*
State Vector 2	*statev2*
UTC parts	*UTC_parts* (= 7)
FOV (footprint) vertices	*FOV_vertices* (= 4)
Dimension label	**Definition (C-order)**
1D	(*atrack*)
2D	(*atrack*, *xtrack*)
2Du	(*atrack*, *UTC_parts*)
3Dv	(*atrack*, *xtrack*, *FOV_vertices*)
4D	*(atrack, xtrack, statev1, statev2*)

2.2.5.1 *Geometry* group

The *Geometry* data group consists of all timing, observation geometry, and geolocation variables produced during Level 1B processing (see Table 2-3). This data group and its contents will be replicated within any relevant downstream product (e.g., Level 2 data products), rather than stored as a separate geometry file.

Users of NetCDF software packages that try to automatically decode times should be aware that these packages may incorrectly interpret the *ctime* variable as a UTC time. The *ctime* variable is a count of total fractional SI seconds since the epoch 2000-01-01T00:00:00 UTC (i.e., no leap second adjustments since that epoch), while the UTC time standard is adjusted to account for all leap seconds. For example, when the PREFIRE *Geometry* group is read by the open_dataset function of the Python xarray package using the default decode_times=True argument, the resulting *ctime* values (with datetime64 data type) will differ from the *time_UTC_values* variable by the number of leap seconds that occurred between 2000-01-01T00:00:00 UTC and the observation time. Users of xarray and other packages that exhibit this behavior are recommended to use *ctime* along with *ctime_minus_UTC* to calculate UTC times if desired, and/or consult *time_UTC_values* to verify the correct UTC timestamps of PREFIRE observations.

For example, for an xarray dataset, a datetime64 DataArray could be computed as follows:

```
import xarray as xr
ds = xr.open_dataset({path_to_1B-RAD_product}, group='Geometry')
ds['UTC_dt64'] = ds['ctime'] – ds['ctime_minus_UTC']
```

Further details on the handling of leap seconds in the CF NetCDF Metadata Conventions can be found in Section 4.4.1 of the CF-1.9 Conventions: https://cfconventions.org/Data/cf-conventions/cf-conventions-1.9/cf-conventions.html#calendar.

Table 2--3

Variable Name	**Type**	**Dimen-sion**	**Units**	**Description**
obs_ID	int64	2D		unique integer identifier for each TIRS look YYYYMMDDhhmmsstbd, composed of UTC date (YYYYMMDD) and time (hhmmss) at TIRS image integration midpoint, t = tenths of seconds [0–9], b = satellite number [1–2], d = scene number [1–8]
ctime	float64	1D	seconds	continuous time since the epoch 2000-01-01T00:00:00 UTC (i.e., similar to TAI) at the midpoint of each TIRS image integration
ctime_minus_UTC	int8	1D	seconds	continuous time minus UTC (i.e., leap seconds since the ctime epoch) at the midpoint of each TIRS image integration
time_UTC_values	int16	2Du	various	UTC datetime at the midpoint of each TIRS image integration, represented as an integer array.

				Array parts: year, month, day, hour, minute, second, millisecond
latitude	float32	2D	degrees_ north	topography-corrected latitude of FOV centroid
longitude	float32	2D	degrees_ east	topography-corrected longitude of FOV centroid
vertex_latitude	float32	3Dv	degrees_ north	topography-corrected latitude for each of the four vertices/corners (arranged counterclockwise starting at the trailing-left corner) of a 4-sided polygon that closely approximates the geolocated FOV (orbital motion taken into account)
vertex_longitude	float32	3Dv	degrees_ east	topography-corrected longitude for each of the four vertices/corners (arranged counterclockwise starting at the trailing-left corner) of a 4-sided polygon that closely approximates the geolocated FOV (orbital motion taken into account)
land_fraction	float32	2D		land_area / total_area (remainder is water_area) within the FOV, according to the Digital Elevation Model (DEM)
elevation	float32	2D	m	mean topographic elevation within the FOV
elevation_stdev	float32	2D	m	standard deviation of topographic elevation within the FOV
viewing_zenith_angle	float32	2D	degrees	viewing zenith angle at the FOV centroid
viewing_azimuth_angle	float32	2D	degrees	viewing azimuth angle at the FOV centroid (zero is north, clockwise-positive looking down from the zenith)
solar_zenith_angle	float32	2D	degrees	solar zenith angle at the FOV centroid
solar_azimuth_angle	float32	2D	degrees	solar azimuth angle at the FOV centroid (zero is north, clockwise-positive looking down from the zenith)
solar_distance	float64	2D	km	distance from FOV centroid to the solar barycenter
subsat_latitude	float32	1D	degrees_ north	sub-satellite latitude
subsat_longitude	float32	1D	degrees_ east	sub-satellite longitude
sat_altitude	float32	1D	km	satellite altitude above the reference ellipsoid (at the sub-satellite point)
sat_solar_illumination_flag	int8	1D		flag specifying whether the spacecraft is illuminated by the sun; 0=no, 1=partial, 2=full
geoloc_quality_bitflags	uint16	2D		integer composed of bit flags that contain info about the quality of the overall geolocation of each along-track

				frame of scenes
maxintgz_verts_lat	float32	3Dv		latitude (topography-corrected) for each of the four vertices/corners (arranged counterclockwise starting at the trailing-left corner) of a 4-sided polygon that closely approximates the geolocated zone with the maximum TIRS image integration time
maxintgz_verts_lon	float32	3Dv		longitude (topography-corrected) for each of the four vertices/corners (arranged counterclockwise starting at the trailing-left corner) of a 4-sided polygon that closely approximates the geolocated zone with the maximum TIRS image integration time
orbit_phase_metric	float32	1D	degrees	orbit phase angular metric (range of 0-360 degrees, varying approximately linearly with time), defined as 0 deg at the ascending node (northward equator crossing) of the satellite orbit, 180 deg at the descending node, and so on
satellite_pass_type	int8	1D		flag specifying which type of satellite pass each frame is mostly/all part of. −1 = descending, 1 = ascending

2.2.5.2 *Cld* group

Table 2--4

Variable Name	Type	Dimension	Units	Description
cloud_d_eff	float32	2D	um	retrieved cloud particle effective diameter
cloud_d_eff_unc	float32	2D	um	uncertainty of retrieved cloud particle effective diameter
cloud_d_eff_prior	float32	2D	um	cloud particle effective diameter prior used to begin the retrieval
cloudtop_pressure	float32	2D	hPa	retrieved air pressure at the cloud top
cloudtop_pressure_unc	float32	2D	hPa	uncertainty of retrieved cloud-top air pressure
cloudtop_pressure_prior	float32	2D	hPa	cloud-top air pressure prior used to begin the retrieval
cloud_tau	float32	2D		retrieved cloud optical depth
cloud_tau_unc	float32	2D		uncertainty of retrieved cloud optical depth
cloud_tau_prior	float32	2D		cloud optical depth prior used to begin the retrieval

posterior_covariance	float32	4D		Posterior covariance
averaging_kernel_matrix	float32	4D		Averaging Kernel information content
reduced_chi_squared_at_start	float32	2D		reduced chi squared at the prior state
reduced_chi_squared	float32	2D		reduced chi squared at the retrieved state
iterations	int8	2D		number of iterations
diverging_steps	int8	2D		number of diverging steps
cld_quality_flag	int8	2D		flag specifying the overall quality of the CLD retrieval for each scene [0] best retrieval, [1] good retrieval (retrieval converged but did not meet quality check), [2] retrieval did not converge, [3] retrieval went out of range
cld_qc_bitflags	uint16	2D		bit flags that contain additional detail about the quality of the CLD retrieval/fields [b0] reduced chi squared is over threshold, [b1] retrieval exceeded iteration limit, [b2] retrieval exceeded divergence limit, [b3] retrieval went out of range, [b4] retrieval solver crashed, [b12] retrieval not attempted due to cloud mask, [b13] retrieval not attempted due to latitude constraint, [b14] retrieval not attempted due to 1B-RAD status

3 Updates Since Previous Version

None – this is the initial version.

4 Known Issues

The 2B-CLD algorithm produces the same product for all scenes and for both instruments. However, it is important to keep in mind that the information content for each scene will be unique due to instrument-specific channel center frequencies and differences in the number of channels used for each cross-track scene retrieval.

The 2B-CLD algorithm retrieves cloud properties assuming that the cloud consists of predominantly ice, meaning that there are possible increases in bias and uncertainties when cloud liquid water is present.

The estimated spectral response functions (SRFs) are known to have minor mismatches compared to instrument performance, and the resultant radiance biases could impact the 2B-CLD retrievals. In 2B-ATM the radiance biases per channel have been characterized as a function of surface temperature and corrections for those have been implemented in clear-sky scenes. The impact of the differences in the modeled and measured radiances in cloudy scenes has not been quantified.

There are instances where the retrieval is not sufficiently constrained – for example, one of the state variables may go outside of a physically reasonable range during iteration. The out-of-range condition halts iteration, which implies an unphysical value is present in the retrieval (for example, negative CTP). These retrievals can be identified with the *cld_quality_flag* (Tables 2-1 and 2-4). Any time a state variable steps out of the physical limits it is indicated via the *cld_quality_flag* field with a value of 3. Initial investigation suggests that this out-of-range condition occurs for about 15-20% of FOVs.

It is currently recommended to use *cld_quality_flag* = 0 when determining the "good" data (i.e., from the most-robust retrievals), although these are more limited in occurrence. FOVs with *cld_quality_flag* = 1 may have specific issues (such as a misclassified sky condition from 2B-MSK).

Geolocation:

The GPS receiver on PREFIRE-SAT1 has performed poorly since launch, and the GPS receiver on PREFIRE-SAT2 ceased to function as well at the end of August 2024. Because of the lack of continuously reliable GPS position and time data, the time-dependent orbital position and velocity vectors used for geolocation are based on orbital reconstructions. This uses publicly available orbit element sets (e.g., Two-Line Element sets (TLEs) based on ranging observations by the United States Space Force and other entities. The precision and accuracy of the orbit reconstruction is currently undergoing evaluation. In addition, residual uncertainties exist due to pointing offsets from lack of precise knowledge of the spectrometer slit orientation relative to the spacecraft. These uncertainties will be addressed after the orbit reconstruction is evaluated and optimized. The current best estimate is that individual geolocated scenes could have along-track geolocation errors of up to 50 km with an average of approximately 30 km (less than the along-track dimension of a ground footprint). The cross-track geolocation error has not been quantified, but the error is likely to be less than the cross-track scene width (approximately 12 km), based on favorable spatial correlations with co-located geostationary imagery collected in the MIR atmospheric window.

As more PREFIRE-TIRS data are collected and analyzed, the quantification of the geolocation biases will improve. Further refinements of the geolocation algorithm are planned, which will reduce these errors in future 1B-RAD data product releases.

Electronic pattern noise:

Electrical cross talk between adjacent FPA detectors was largely mitigated by alternating the wiring polarity in the readout integrated circuits. However, residual pattern noise has been noted in both the raw data and the calibrated radiances. This noise is highly temporally correlated and impacts all spectral channels.

This electrical noise manifests in two primary ways. First, "sawtooth-like" patterns can be visible in an individual spectral observation, where the even and odd spectral channels have different radiometric biases. These patterns are generally visible in spectral residuals (observation – modeled radiance). Due to the temporal correlation this pattern could be visible in multiple consecutive frames. Second, "striping" is visible when data from a selected channel are viewed spatially, where specific spatial scenes are clearly biased relative to the other scenes. Again, due to the temporal correlation these stripes will continue along track for some time. No data flagging is performed related to this pattern noise effect, but future developments in the calibration algorithm are planned to further reduce this noise.

5 Resources

The Algorithm Theoretical Basis Document (ATBD) can be found at https://prefire.ssec.wisc.edu/Documents/PREFIRE_2B-CLD_ATBD.pdf. For more information, contact Erin Hokanson Wagner at prefire-sdps.admin@office365.wisc.edu.

6 References

L'Ecuyer, T.S., Drouin, B.J., Anheuser, J., Grames M., Henderson, D., Huang, X., Kahn, B.H., Kay, J.E., Lim, B.H., Mateling, M., Merrelli, A., Miller, N.B., Padmanabhan, S., Peterson, C., Schlegel, N.-J., White, M.L., Xie, Y., "The Polar Radiant Energy in the Far-InfraRed Experiment: A New Perspective on Polar longwave Energy Exchanges," *Bulletin of the American Meteorological Society (BAMS*), 102(7), E1431–E1449, 2021.

Liu, X., Smith, W.L., Zhou, D.K., Larar, A., 2006. Principal component-based radiative transfer model for hyperspectral sensors: theoretical concept. Appl. Opt. 45, 201–209.

Padmanabhan, S., Drouin, B., L'Ecuyer T., White, M., Lim. B., Kenyon, M., Mariani, G., McGuire J., Raouf, N., De Santos, O., Bendig, R., "The Polar Radiant Energy in the Far-InfraRed Experiment (PREFIRE)," *IGARSS 2019 – 2019 IEEE International Geoscience and Remote Sensing Symposium*

Rodgers, C. (2000) Inverse Methods for Atmospheric Sounding: Theory and Practice. World

Scientific Publishing Co Pte. Ltd.

Citation

DOI:

- PREFIRE_SAT2_2B-CLD_R01: 10.5067/PREFIRE-SAT2/PREFIRE/CLD_L2B.R01
- PREFIRE_SAT1_2B-CLD_R01: TBD